

PREPARED FOR SUBMISSION TO JINST

1ST WORKSHOP ON NEW FRONTIERS IN LEPTON FLAVOUR

15 - 17TH MAY 2023

PISA, ITALY

Measuring tau g-2 using ATLAS Pb+Pb collisions

W. Stanek-Maslouska on behalf of the ATLAS collaboration

Deutsches Elektronen-Synchrotron DESY,

Notkestr. 85, 22607 Hamburg, Germany

E-mail: veronika.stanek@desy.de

ABSTRACT: Relativistic heavy-ion beams at the LHC are accompanied by a large flux of equivalent photons, leading to photon-induced processes. Measurements of photon-induced production of tau lepton pairs can be used to constrain the tau lepton's anomalous magnetic dipole moment ($g-2$). A recent ATLAS measurement using muonic decays of tau leptons in association with electrons and tracks is presented. This provides one of the most stringent limits on $g-2$ of the tau lepton to date.

KEYWORDS: ultra-peripheral heavy-ion collisions, heavy ions, tau leptons, tau $g-2$, magnetic moment



Contents

1	Introduction	1
2	Experimental realisation	1
3	Observation of $\gamma\gamma \rightarrow \tau\tau$ in Pb+Pb	2
4	Conclusions	3

1 Introduction

Measurements of anomalous magnetic moments of leptons $a_\ell = \frac{1}{2}(g_\ell - 2)$ are foundational tests of the Standard Model (SM) and a powerful tool to investigate beyond the SM (BSM) physics, for instance lepton compositeness or supersymmetry [1].

In the case of electrons and muons, their anomalous magnetic moments are some of the most precisely measured observables in nature [2, 3], however, a_τ is still much less constrained ($-0.052 < a_\tau < 0.013$) [4]. This is mainly due to the short τ -lepton lifetime which renders experimental challenges.

In this study $\text{Pb+Pb} \rightarrow \text{Pb}(\gamma\gamma \rightarrow \tau\tau)\text{Pb}$ is observed using 1.44 nb^{-1} of $\sqrt{s_{\text{NN}}} = 5.02 \text{ TeV}$ Pb+Pb data recorded by the ATLAS detector [5] in 2018. Ultra-peripheral collisions (UPC) were utilised, in which the distance between two incoming nuclei is larger than twice the ion radius. This results in interactions between strong electromagnetic fields, which gives rise to photon induced processes. This approach has numerous advantages over photon-photon interactions in proton-proton collisions, for example Z^4 cross-section enhancement ($Z = 82$ for Pb) and a clean environment with low transverse momentum (p_{T}) thresholds in the trigger and offline reconstruction [1].

2 Experimental realisation

Signal samples were simulated using the STARLIGHT 2.0 Monte Carlo (MC) generator [6], interfaced with TAUOLA [7] for the τ -lepton decays and PYTHIA 8.245 [8] for final-state radiation. The photon-flux distribution was re-weighted to SUPERCHIC 3.05 [9]. Signal candidates were selected using muonic τ decays and categorised using electrons or low- p_{T} tracks into three signal regions (SRs): $\mu 1\text{T-SR}$ (muon + 1 track), $\mu 3\text{T-SR}$ (muon + 3 tracks) and $\mu e\text{-SR}$ (muon + electron). In order to reduce the systematic uncertainties, an additional di-muon control region ($2\mu\text{-CR}$) was introduced [10, 11].

The two main sources of background after event selection are photon induced di-muon and photonuclear events. The former is estimated using STARLIGHT and PYTHIA8 (MADGRAPH [12] in the case of radiative di-muon background) MC generators with the photon-flux distribution re-weighted to SUPERCHIC. The estimation of the latter involves a data-driven method in which additional CR are built, similar to the SRs but with the requirement of an additional low- p_{T} track.

The analysis strategy is to exploit the $\gamma\gamma \rightarrow \tau\tau$ cross-section dependence and muon p_{T} shape dependence on a_τ . A fit to the muon p_{T} distribution in the SRs and CR is performed to extract the value of a_τ .

3 Observation of $\gamma\gamma \rightarrow \tau\tau$ in Pb+Pb

The observation of $\gamma\gamma \rightarrow \tau\tau$ in Pb+Pb collisions is established with a significance exceeding 5 standard deviations. The significance is the highest in the $\mu 1T$ -SR, while the largest signal-background ratio is observed in the μe -SR.

The signal strength is defined as a ratio of the observed signal yield to the SM prediction, assuming the SM value of a_τ . It is calculated using a profile-likelihood fit with $\mu_{\tau\tau}$ being the only parameter of interest. It is measured to be $\mu_{\tau\tau} = 1.03^{+0.06}_{-0.05}(\text{tot}) = 1.03^{+0.05}_{-0.05}(\text{stat.}) = 1.03^{+0.03}_{-0.03}(\text{syst.})$.

In order to measure a_τ , a profile likelihood fit in the three SRs and 2μ -CR is used, in which a_τ is the only free parameter. The distribution of p_T^μ is chosen because of its high sensitivity to a_τ . Templates with different a_τ values are employed and in the nominal signal sample a_τ is set to the SM value ($a_\tau^{\text{SM}} = 0.00117721(5)$) [13]. Samples with different a_τ hypotheses are obtained by reweighting the nominal sample in three-dimensions ($\tau\tau$ invariant mass, rapidity and difference in pseudorapidity between the two τ -leptons) [11]. This parametrisation matches the one used in previous LEP measurements [4, 14, 15]. In total, 14 samples with different a_τ values are employed.

Pre-fit and post-fit distributions of p_T^μ in the $\mu 1T$ -SR are presented in Fig. 1. The fit describes the data well and the uncertainties evidently decrease in the post-fit distribution (as shown in the ratio panel). Differences between SM and BSM values of a_τ depend on muon p_T .

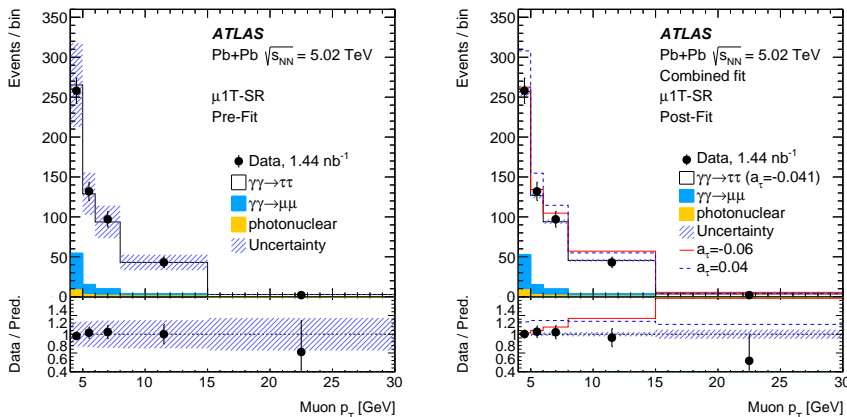


Figure 1. Pre-fit (left) and post-fit (right) muon transverse momentum distributions in the $\mu 1T$ signal region. Black markers denote data and stacked histograms indicate the different components contributing to the signal region. Post-fit distributions are shown with the signal contribution corresponding to the best-fit a_τ value ($a_\tau = -0.041$) [1].

The best-fit a_τ value is measured to be $a_\tau = -0.041$ with the corresponding 68% and 95% confidence levels (CL) being $(-0.050, -0.029)$ and $(-0.057, 0.024)$, respectively. The results of the a_τ measurements compared to the previous results obtained by LEP [4, 14, 15] are presented in Fig. 2. The expected 95% CL limits from the combined fit are $-0.039 < a_\tau < 0.020$. The highly asymmetric 95% CL interval is due to the higher than expected observed yields and the nearly quadratic cross-section dependence on a_τ which arises due to interference of SM and BSM amplitudes [10, 11]. The precision of the measurement is competitive with previous electron-collider studies, however, the study is strongly limited by the statistical uncertainties which are significant in comparison with systematic uncertainties.

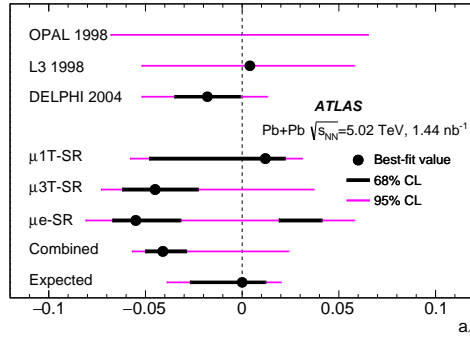


Figure 2. Results of a_τ measurement from fits to individual signal regions (and the di-muon control region), and from the combined fit, compared with existing measurements conducted at LEP [4, 14, 15]. A point denotes the best-fit a_τ value for each measurement if available, while thick black (thin magenta) lines show 68% (95%) confidence level intervals [1].

4 Conclusions

The observation of τ -lepton production in UPC Pb+Pb collisions in the ATLAS detector was established with a significance exceeding 5 standard deviation using 1.44 nb^{-1} of $\sqrt{s_{\text{NN}}} = 5.02 \text{ TeV}$ data, which indicates that UPCs can be used to probe rare SM processes and search for BSM phenomena. This opens hadron-collider studies to measure electromagnetic τ properties. The obtained constraints on a_τ are competitive with previous electron collider results.

Copyright 2023 CERN for the benefit of the ATLAS Collaboration. Reproduction of this article or parts of it is allowed as specified in the CC-BY-4.0 license

References

- [1] ATLAS Collaboration, (2022), [arXiv:2204.13478 \[hep-ex\]](#)
- [2] Odom, B. et al., *Phys. Rev. Lett.* **97** (2006) 030801
- [3] Abi, B. et al., *Phys. Rev. Lett.* **126** (2021) 141801
- [4] DELPHI Collaboration, *EPJC* **35** (2004) 159
- [5] ATLAS Collaboration, *JINST* **3** (2008) S08003
- [6] Klein, S. R. et al., *Comput. Phys. Commun.* **212** (2017) 258
- [7] Jadach, S. et al., *Comput. Phys. Commun.* **76** (1993) 361
- [8] Sjöstrand, T. et al., *Comput. Phys. Commun.* **191** (2015) 159
- [9] Harland-Lang, L. A. et al., *Eur. Phys. J. C* **79** (2019) 39
- [10] Beresford, L. and Liu, J., *PRD* **102** (2020) 113008
- [11] Dyndał, M. et al., *PLB* **809** (2020) 135682
- [12] Alwall, J. et al., *JHEP* **07** (2014) 079
- [13] Eidelman, S. and Passera, M., *Mod. Phys. Lett. A* **22** (2007) 03
- [14] OPAL Collaboration, *Phys. Lett. B* **431** (1998) 188
- [15] L3 Collaboration, *Phys. Lett. B* **434** (1998) 169